Brain Hemodynamics

15

Nathan Gaines and David S. Liebeskind

Abstract

Revision of the fundamental pathophysiology of cerebral ischemia may seem unwarranted, yet advances in stroke imaging and therapeutics over the last 30 years have revolutionized our understanding of basic tenets in the field. Brain hemodynamics remains a poorly understood area of basic pathophysiology with tremendous implications for the clinical management of cerebrovascular disease. Early descriptions by Astrup et al. in the 1980s of thresholds for cerebral ischemia and the ischemic penumbra (Astrup et al., Stroke 12(6):723–725, 1981) in stroke remain the predominant framework for acute stroke pathophysiology. This idealized model captures the basic principles of ischemia well: there are thresholds of cerebral blood flow (CBF) through which cells progress stepwise from dysfunctional but viable to irreversibly damaged and, ischemic stroke typically has a core region of irreversibly infarcted tissue with a surrounding region of salvageable tissue known as the penumbra. In the intervening decades, however, advances in neuroimaging and clinical management of stroke have forced reconsideration of the greater complexities of CBF and cerebral ischemia. While this earlier model presents a fairly static situation, in practice, clinicians encounter a dynamic process, with numerous variables affecting the clinical outcome, perhaps most notably, the option for therapeutic revascularization that was developed after the model was published. The major ongoing challenge for acute stroke management is that current therapies, i.e., intravenous tissue plasminogen activator (tPA) and endovascular thrombectomy, risk not only futility if administered too late, but may cause additional harm through reperfusion injury and hemorrhagic conversion in a subset of cases. Better understanding of the complex interactions between patient-specific variables affecting CBF is therefore essential for effective and safe precision medicine in stroke.

Rather than emphasizing the more theoretically straightforward models of cerebral hemodynamics and stroke, this chapter will focus on advanced multimodal neuroimaging and emerging understanding of the complexities of CBF pathophysiology such as collaterals, microcirculation, and venous hemodynamics that underlie the wide variance encountered in clinical practice. While there are numerous clinical situations that deserve careful discussion of brain hemodynamics, for clarity this chapter will primarily focus on cerebral blood flow as it relates to ischemic stroke.

N. Gaines · D. S. Liebeskind (✉)
UCLA Department of Neurology, University of California, Los Angeles Medical Center, Los Angeles, CA, USA
e-mail: DLiebeskind@mednet.ucla.edu

© Springer Science+Business Media Singapore 2020

S.-H. Lee (ed.), *Stroke Revisited: Pathophysiology of Stroke*, Stroke Revisited,
https://doi.org/10.1007/978-981-10-1430-7_15

15.1 Hemodynamics of Cerebral Blood Flow

15.1.1 Normal Hemodynamics and Autoregulation

Cerebral hemodynamics remain an unsolved area of investigation; traditional laboratory thresholds for both normal values and for cellular dysfunction and ischemic infarction are complicated by numerous factors encountered in clinical practice. The influence of age, time, blood pressure, medical comorbidities, therapeutic interventions, and other variables on the complex processes of autoregulation, collaterals, microcirculation, venous outflow, and cellular dysfunction versus cell death remains a work in progress. Genuine understanding of cerebral hemodynamics will require an integrated model for these complex interactions; at present, no such model exists.

Cerebral blood flow (CBF) is defined as the cerebral perfusion pressure (CPP) divided by the cerebrovascular resistance (CVR):

$$\mathrm{CBF} = \mathrm{CPP} / \mathrm{CVR}$$

CPP is the difference between mean arterial pressure (MAP) and intracranial pressure (ICP):

$$\mathrm{CPP} = \mathrm{MAP} - \mathrm{ICP}.$$

Apart from circumstances with elevated ICP or extremes of MAP, CBF is determined by CVR, which is a product of vessel radius, vessel length, and blood viscosity. Since the cerebral vasculature lacks the precapillary sphincters that primarily regulate vascular resistance in the peripheral vasculature, the dominant mechanism for regulating CBF is through changing the intraluminal diameter of the arteries and arterioles [1].

The major physiologic drivers of change in CVR are carbon dioxide, oxygen [2, 3], as well as myogenic, neurogenic, and endothelial mechanisms (e.g., nitrous oxide) [4]. Changes in carbon dioxide are more potent than those of oxygen. CBF does not change significantly until pO_2 falls to about 30–50 mmHg [5], while voluntary hyperventilation to drive down pCO_2 produces vasoconstriction with CBF reductions of 30–35% and inhaling CO_2 results in vasodilation and increased CBF by up to 75% [2, 3].

Under normal circumstances, autoregulation is highly effective in maintaining stable CBF over a wide range of CPP; at least 70–150 mm Hg [6]. The autoregulatory curve can shift based on chronic illness, acute disease states, and acute CNS insults, among other factors. For example, chronic hypertension shifts the entire curve to the right such that higher CPP is tolerated before CBF increases but CBF can begin to fall at typically normotensive MAP levels that would be tolerated in non-hypertensive individuals [7]. The shape of the curve can also be changed in certain disease states with shrinking of the normal autoregulatory zone (e.g., subarachnoid hemorrhage, bacterial meningitis, critically elevated intracranial pressure). In extreme circumstances of complete autoregulatory failure the curve may even behave in a linear fashion such that changes in CPP and CBF are matched (Fig. 15.1).

Early investigations produced the common wisdom that autoregulation is regionally impaired following stroke; however, the findings of subsequent studies are more nuanced. Two forms of cerebral autoregulation are recognized: dynamic and static. Dynamic autoregulation refers to rapid changes in blood pressure over seconds. Static autoregulation involves the response to more prolonged, steady-state changes in blood pressure. In stroke, dynamic autoregulation is impaired throughout the acute and subacute period, with changes affecting ipsilateral and contralateral brain hemispheres and present even in small strokes [4]. The clinical implications of reduced dynamic autoregulation are unclear. However, preservation of static autoregulation has been demonstrated in several small studies by introducing antihypertensive medications to reduce MAP in the acute and subacute period after stroke, with no significant impairment of regional autoregulation being observed [8–10]. One explanation for discrepancies in the data is that earlier studies focused on vasomotor reactivity to agents such as inhaled CO_2 and acetazolamide as a surrogate measure of autoregulation. While vasomotor reactivity is impaired or even absent following

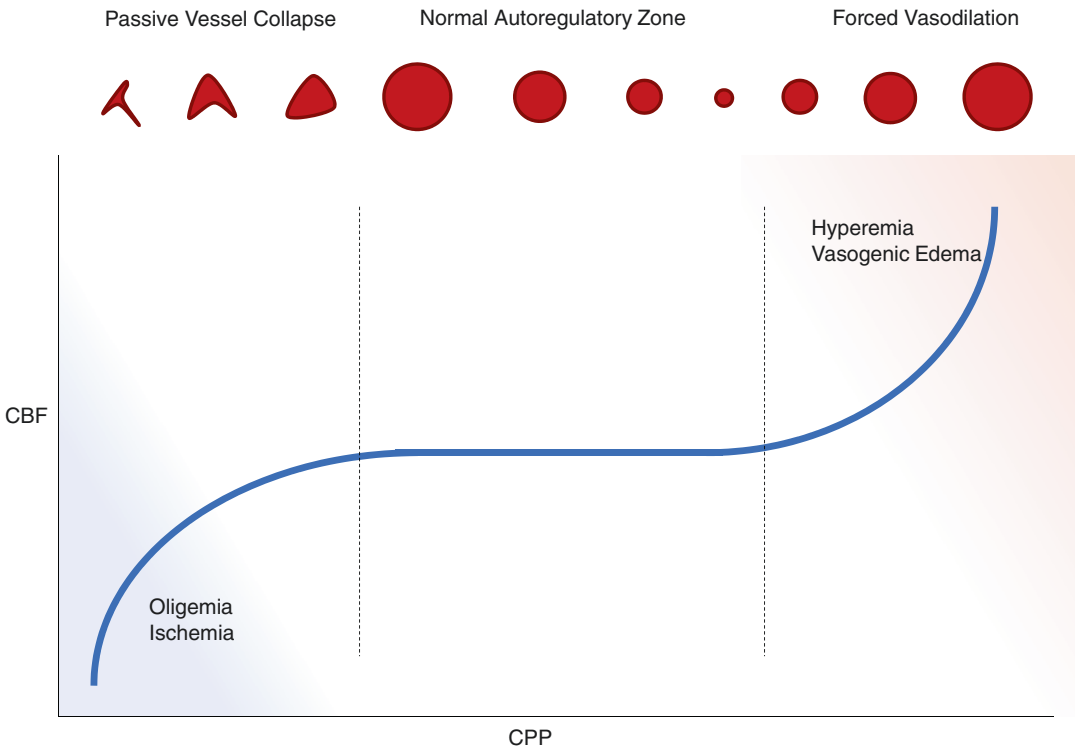

Fig. 15.1 Autoregulatory curve

stroke, subsequent studies have demonstrated that vasomotor reactivity and autoregulation are in fact distinct processes [4, 11]. It appears from these data that steady reductions in MAP affecting static autoregulation may not directly result in impaired CBF in cerebral tissue at risk, at least for some patients, but the findings are not definitive.

It is clinically important to recognize, however, that several circumstances common to stroke patients do impair autoregulation. The rightward shift of the autoregulatory curve in chronically hypertensive patients as well as impaired regional CPP due to persistent arterial occlusion or locally elevated ICP are two common situations in which reduction in MAP could lead to progressive ischemia. It is also important to recognize that the limits of autoregulation are absolute. For example, hypercapnia cannot produce additional vasodilation if it has already been maximized by decreased CPP and vice versa. Consequently, underlying anemia, hypercapnia, or hypoxemia may exhaust the autoregulatory potential [12, 13].

15.1.2 Hemodynamic Failure in Cerebrovascular Disease

There are several models of hemodynamic failure but none capture the complexities of clinical practice. One such model uses a three-stage classification system to describe hemodynamic failure in arterial occlusion or stenosis [14]. Stage 0 applies when CPP remains normal, CBF is preserved, and responses to arteriolar vasodilatory stimuli are intact. Cerebral blood volume (CBV), mean transit time (MTT) are preserved (see the following section for definitions). Stage I, hemodynamic compromise, describes decreased CPP and increased MTT with CBF maintained through compensatory arteriolar vasodilation resulting in increased CBV; oxygen extraction fraction remains normal. Stage II, known as

"misery perfusion" or hemodynamic failure, results when CPP falls below the autoregulatory range and increased oxygen extraction is required to maintain a relatively preserved cerebral metabolism. The utility of this model is limited as there are too many exceptions to the imaging findings it predicts.

More generally, traditional observational studies of hemodynamic failure in stroke describe a fall in CBF that is offset metabolically by a compensatory increase in the oxygen extraction fraction, paired with decreased cerebral oxygen metabolism [15]. Dynamic variations in CBF occur in the initial hours following stroke [16], but eventually some areas of high oxygen extraction will infarct while other survive [17, 18]. A state of "luxury perfusion" may result after reperfusion that describes the subsequent rise in CBF through abnormally dilated vessels due to elevated pCO_2 in the area of infarction, but with persistently low cerebral metabolism and oxygen extraction. In the absence of therapeutic recanalization, the timing of spontaneous reperfusion is variable but peaks around 14 days [19]. In chronic infarction, CBF gradually declines to match the low levels of cerebral metabolism [20].

Typical thresholds for CBF corresponding to neuronal dysfunction (<20 ml/100 g/min) and cell death (<10 ml/100 g/min) have been described in animal models [21], but standard values and clinical outcomes vary in numerous ways, rendering such measures more theoretical than clinically applicable. CBF ischemic thresholds in humans are more variable, ranging from 4.8 to 8.4 ml/100 g/min [22]. Different cell types are more susceptible to ischemic infarction with gray matter being more vulnerable [23, 24] as is seen in typical infarction patterns from global cerebral hypoperfusion, which preferentially affects the basal ganglia, thalami, cerebral cortex, cerebellum, and hippocampi. Cellular dysfunction and cell death are a product of both the degree and duration of ischemia; i.e., brief severe ischemia may cause no lasting damage while persistent moderate CBF impairment can result in infarction. Various factors appear to modify the severity of stroke: observational studies suggest modest improvement in outcomes related to statin use prior to stroke [25], remote ischemic preconditioning [26], body temperature, and even smoking [27] among many other factors, further highlighting the complex variability of tissue outcomes.

Disruption of neurologic function in viable brain tissue due to cerebral hypoperfusion is recognized in the penumbral area of acute ischemic stroke, but clinical dysfunction can also result from chronic sub-ischemic impairment in CBF. One prominent example is the finding that cognitive dysfunction in moyamoya disease correlates with hypoperfusion to frontal and parietal lobes similar to patients with frontal and parietal lesions [28]. In another study, revascularization with burr hole surgery improved cerebral perfusion markers on MRI, leading to complete resolution of cognitive impairments in adults with moyamoya disease [29].

15.1.3 Collateral Circulation

The collateral circulation plays a pivotal role in the pathophysiology of cerebral ischemia, but knowledge of how this complex and highly variable system functions remains limited. During arterial insufficiency, collateral flow pathways can be recruited to compensate for reduced CBF through primary and secondary pathways. The primary pathways are those in the circle of Willis, but it is complete in only a minority of cases. Common variants include absence or hypoplasia of a posterior communicating artery in 30%, anterior cerebral artery in 10%, and anterior communicating artery in 1% (see Fig. 15.2). The major secondary pathways include reversal of flow in the ophthalmic artery, dural and leptomeningeal or pial arteriolar connections to cortical vessels, and anastomoses of distal segments of the major intracranial vessels. These anastomoses are most robust between the anterior cerebral arteries (ACA) and middle cerebral arteries (MCA), less prominent between the MCAs and posterior cerebral arteries (PCA), and sparse between the PCAs and ACAs. Analogous anastomoses exist in the vertebrobasilar and cerebellar circulation [30].

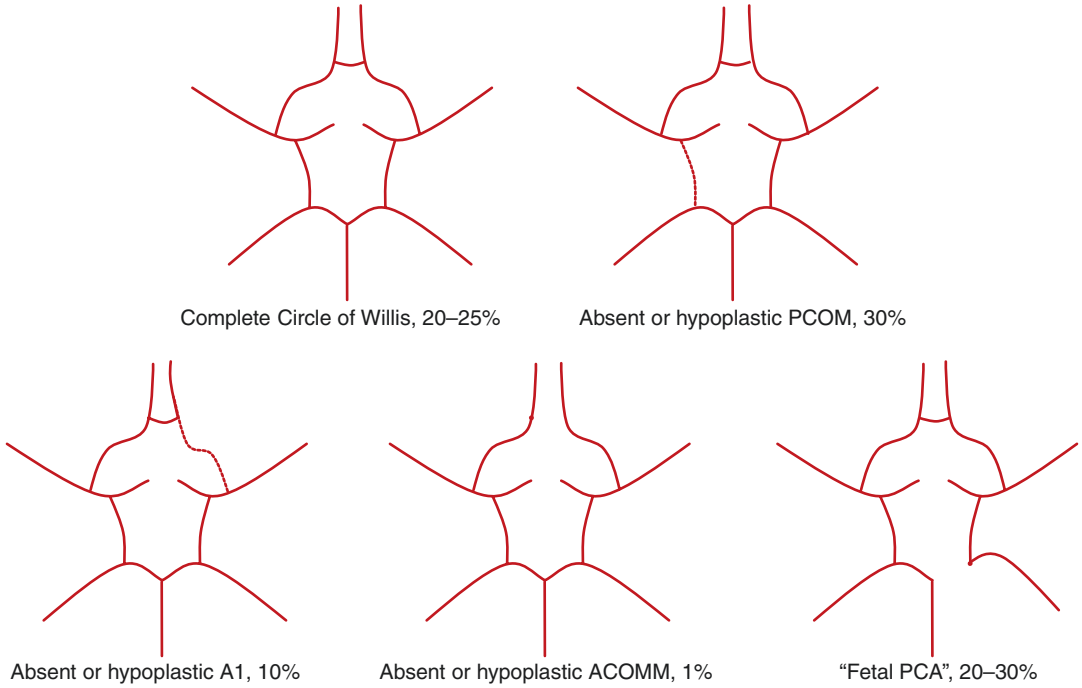

Fig. 15.2 Common circle of Willis variants

While large caliber primary collaterals are able to provide immediate supplementary blood flow, the smaller caliber secondary collateral vasculature may take time to develop sufficient capacity to make a clinically meaningful contribution to tissue at threat of infarction. The exact factors leading to collateral recruitment are poorly understood and likely depend on a combination of hemodynamic, metabolic, and neural mechanisms [30]. Angiogenesis may stimulate collateral growth in the periphery of an ischemic region [31], though these vessels may be recruited for removal of necrotic debris rather than augmenting CBF [32]. Development of collaterals does not guarantee their persistence, and efficacy of collaterals likely depends on patient age, duration of ischemia (i.e., chronic or acute), and comorbid medical illnesses, though exact relationships with these parameters are not yet defined [30] (Figs. 15.3, 15.4, and 15.5).

In acute ischemia, collaterals are important for augmenting CBF, spontaneously clearing thromboemboli, and enhancing access of thrombolytics [33]. The presence of leptomeningeal collaterals

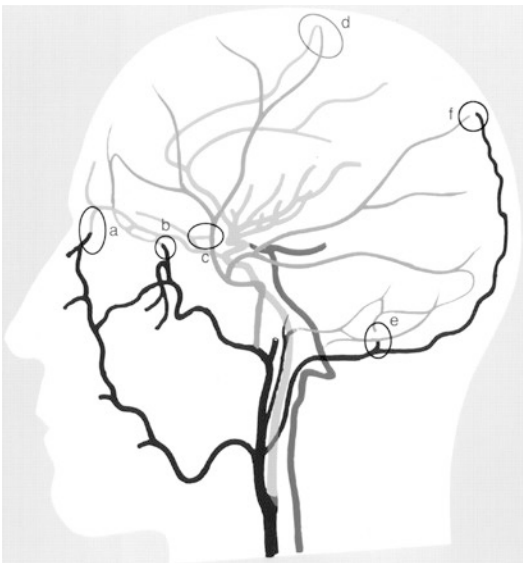

Fig. 15.3 Extracranial arterial collateral circulation. Shown are anastomoses from the facial (a), maxillary (b), and middle meningeal (c) arteries to the ophthalmic artery and dural arteriolar anastomoses from the middle meningeal artery (d) and occipital artery through the mastoid foramen (e) and parietal foramen (f). Stroke 2003;34:2279–2284 [30]

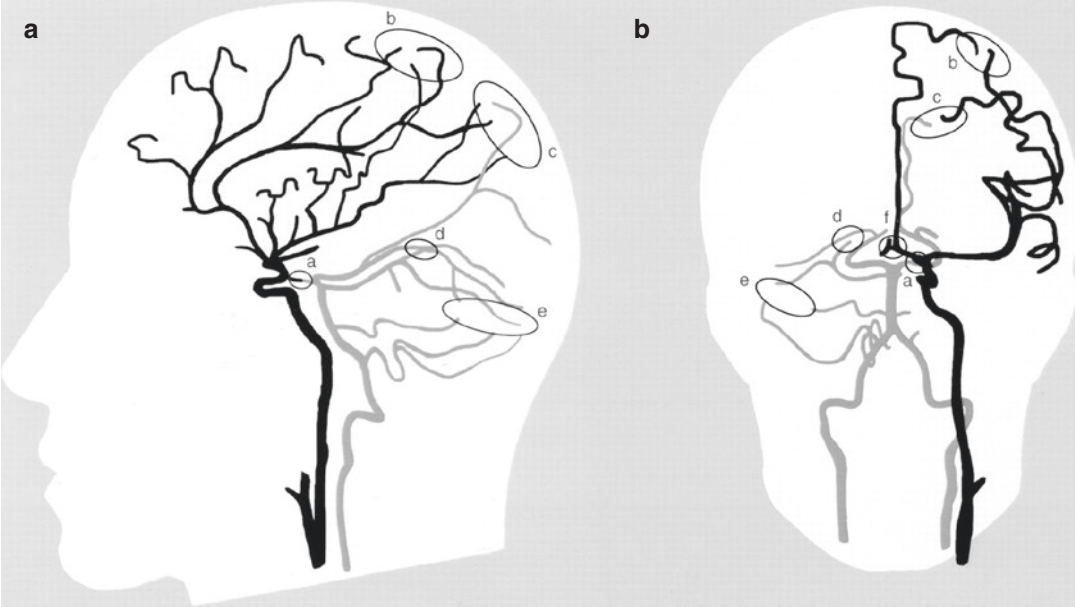

Fig. 15.4 Intracranial arterial collateral circulation in lateral (**A**) and frontal (**B**) views. Shown are posterior communicating artery (a); leptomeningeal anastomoses between anterior and middle cerebral arteries (b) and between posterior and middle cerebral arteries (c); tectal plexus between posterior cerebral and superior cerebellar arteries (d); anastomoses of distal cerebellar arteries (e); and anterior communicating artery (f). Stroke 2003;34:2279–2284 [30]

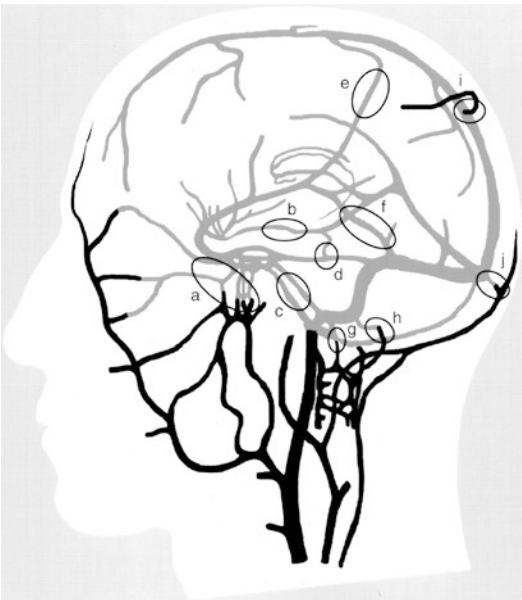

Fig. 15.5 Venous collateral circulation. Shown are pterygoid plexus (a), deep middle cerebral vein (b), inferior petrosal sinus and basilar plexus (c), superior petrosal sinus (d), anastomotic vein of Trolard (e), anastomotic vein of Labbé (f), condyloid emissary vein (g), mastoid emissary vein (h), parietal emissary vein (i), and occipital emissary vein (j). Stroke 2003;34:2279–2284 [30]

predict improved clinical outcomes in MCA occlusion whether or not thrombolytics are given [34]. Therapeutic approaches to enhance collateral formation in acute cerebral ischemia remain unproven at this time, including hypervolemic therapy and permissive or induced hypertension.

Chronic hypoperfusion, such as in progressive carotid artery disease or moyamoya syndrome, has been a major focus of research on collateral development. However, attempts to correlate collateral patterns with hemodynamic and metabolic parameters have so far led to conflicting data. Primary collaterals are assumed to compensate initially with secondary collateral formation gradually occurring as primary collaterals fail; increased secondary collaterals are typically considered a marker of impaired cerebral hemodynamics [30]. The clinical status of patients with disorders causing chronic hypoperfusion (e.g., carotid stenosis) is determined not only by the degree of the primary stenotic lesions, but by the quality of collateral formation. Chronic hypertension has been shown to have an inverse relationship with development of preformed

intracranial collaterals in chronic carotid occlusive disease [35] but the underlying mechanisms for this relationship are unknown. Therapeutic enhancement of collateral circulation is possible in select patients through encephaloduroarteriosynangiosis (EDAS) procedures and has been shown to improve outcomes in pediatric moyamoya disease [36].

15.1.4 Venous Hemodynamics

Despite accounting for about 70% of the cerebral blood volume, the cerebral venous circulation is seldom included in discussions of cerebral hemodynamics, likely because the arterial circulation is both better understood and the site of primary injury in the majority of vascular neurology. Venous pathology likely plays a larger role than previously suspected in cerebrovascular disease. Primary venous pathology is increasingly being recognized thanks to improvements in neuroimaging and higher clinical index of suspicion.

In cases of direct venous dysfunction, such as cerebral venous thromboses, there is even more variation in clinical presentation, baseline anatomy, collateral pathways, and prognosis seen with arterial occlusive disease. Symptoms range from asymptomatic, to mild and nonspecific, to severe neurologic dysfunction and life-threatening disease. As with arterial disease, differentiating patients who warrant aggressive management while avoiding unnecessary therapeutic risk in well compensated patients requires understanding the underlying pathophysiology that informs individualized treatment strategies.

The mechanisms of hemodynamic failure in cerebral venous ischemia differ significantly from arterial disease and are less well understood. Whereas arterial obstruction limits CBF directly, venous congestion underlies impairment of CBF in cerebral vein thrombosis leading to an outflow, rather than inflow problem. Additionally, impairment of CSF drainage via the arachnoid granulations can lead to elevated intracranial pressure. Cerebral dysfunction is the result of a progressive process, starting with increased venous capillary pressure, subsequent impaired drainage and capillary dilation that disrupts the blood–brain barrier and results in extravasation of plasma, and, in severe cases, eventually results in capillary rupture and hemorrhage [37]. Venous infarction results when the combined effect of these changes impairs regional CBF below the regional ischemic threshold. The process may halt and recover spontaneously at any stage, and reversibility of neurologic dysfunction is common due to robust collaterals in the venous system [38, 39]. Cytotoxic and vasogenic edema are seen but in contrast to typical arterial ischemia, structural brain imaging often appears visually worse than the neurologic exam [40]. In a study using time-resolved MRV to evaluate CVT hemodynamics, venous drainage in patients without brain lesions showed sufficient collateral recruitment, while those with brain lesions depended more on drainage through partially occluded outflow tracts [41]. It is also worth noting that venous flow varies by body position: drainage through the internal jugular veins predominate in the supine position (as seen in most angiography studies) but in the upright position the deep venous plexuses such as the vertebral plexus take over [42]—an observation that may have implications both for the interpretation of diagnostic studies and the optimal head positioning of patients with CVT.

15.2 Measurement of Cerebral Blood Flow: Brain SPECT, PET, MRI, and CT

Perfusion imaging represents a major set of tools for precision medicine by helping characterize the state of cerebral blood flow beyond merely identifying occlusions. The various modalities differ significantly and their correct application requires a thorough understanding of the unique advantages and limitations of each technique. There are two major classes of cerebral perfusion imaging techniques: those that use diffusible tracers including positron emission tomography (PET) and single-photon emission computed tomography (SPECT), and those that use nondif-

fusible tracers including CT perfusion (CTP) and magnetic resonance imaging perfusion (MRP).

Each of these attempt to quantify CBF, which, confusingly, also refers to a specific perfusion imaging output parameter in addition to the general concept that is the topic of this chapter. Cerebral blood flow in perfusion imaging is a measure of cerebral blood volume (CBV) over time; CBF = CBV/*t*. Methods for measuring time parameters differ between the imaging modalities, and understanding these differences is necessary for interpreting the results.

15.2.1 SPECT and PET

SPECT and PET are the gold standards for CBF measurement but are too time intensive for acute stroke care and not widely available enough for routine clinical application. These modalities measure absolute CBF by recording regional concentration of radioactive tracers. PET is more reliable for measures of CBF and can also quantify oxygen extraction fraction and cerebral metabolic rate [43]. These modalities are more often used in the research setting and have significantly advanced our understanding of cerebral hemodynamics in stroke and helped identify and define differences between infarcted tissue and dysfunctional tissue at threat, i.e., core and penumbra.

PET and SPECT also uncovered the phenomenon of remote tissue deactivation, or diaschisis, in stroke [43]. This refers to reductions of CBF and cerebral metabolism in brain regions not directly damaged by stroke but functionally related to the involved site. One prominent example is crossed cerebellar diaschisis, seen in lesions involving the corticopontocerebellar pathways; reversibility has been demonstrated following reperfusion therapy [44, 45]. Better understanding of these network phenomena may help explain occasional deviations in the neurologic exam from that expected by "textbook" neuroanatomy in hyperacute neurologic injury.

The ability to measure cerebral metabolism also allows for longitudinal studies showing the patterns of recruitment and compensation in functional networks following stroke [46]. These findings have had implications for stroke rehabilitation, such as the discovery that the unaffected hemisphere may inhibit movement of a paretic limb [47] or language function in patients with aphasia [48], both of which may respond to inhibition of the unaffected hemisphere using transcranial magnetic stimulation [49, 50].

15.2.2 Perfusion MRI and CT

CTP and MRP record the transit of intravascular contrast material through the cerebral vasculature. The primary measures of time used in these modalities are mean transit time (MTT), time to peak (TTP), and time to maximum concentration of the contrast marker (T_{max}). Automated software programs use deconvolution to generate these measures from tissue concentration curves as demonstrated in Fig. 15.6. CBV is derived from the area under the normalized curve. CBF is derived from the CBV and MTT.

MRP can also be performed without the use of an injected contrast material by using the arterial spin labeling technique (ASL). ASL magnetically labels endogenous water molecules in the incoming blood vessels and calculates CBF from changes in labeled blood flowing into the cerebral tissue. Another major advantage of MRI-based perfusion imaging is the ability to pair it with multimodal structural sequences such as diffusion weighted imaging (DWI), susceptibility weighted imaging (e.g., GRE or SWI), and fluid inversion recovery (FLAIR). These structural images aid in understanding the stage of infarction and hemodynamics, in addition to identifying stroke mimics. FLAIR vascular hyperintensities can be another indicator of slow flow through vessels.

15.2.3 Measuring Core and Penumbra

The major clinical application for multimodal neuroimaging in acute stroke management is in identifying clinical-to-imaging mismatch by calculating the amount of irreparably infarcted tis-

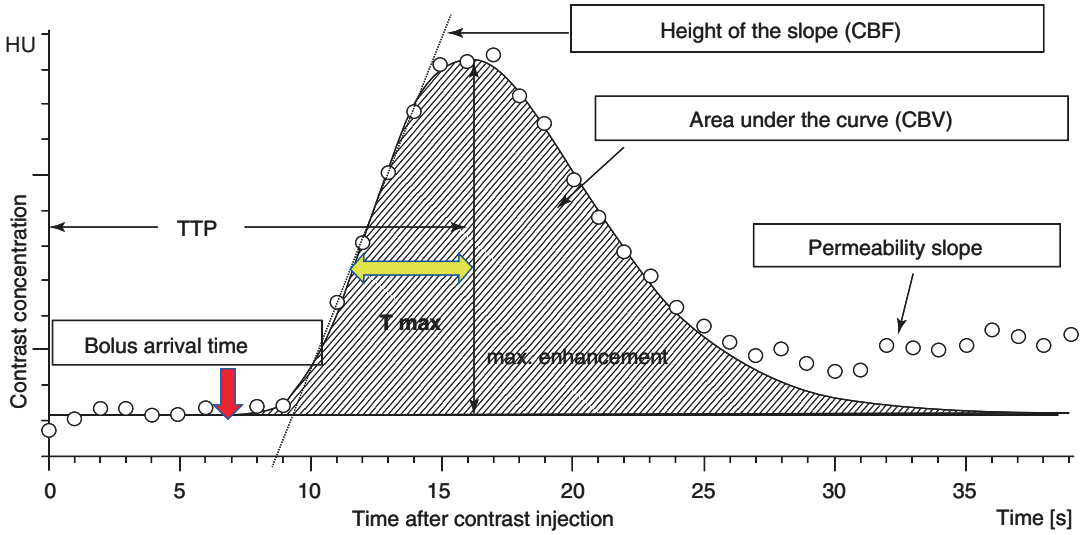

Fig. 15.6 CT perfusion and MRI perfusion tissue concentration curves and CBF parameter derivations. The time to peak (TTP) is measured from the onset of contrast injection to the peak of the deconvolved tissue curve. T_{max} is calculated from the onset to the peak of the deconvolved tissue curve. The cerebral blood flow (CBF) and cerebral blood volume (CBV) are calculated from the height of the curve and the area under the curve, respectively. The presence of "permeability slope" indicates blood–brain barrier disruption. Neuropharmacology. 2018 May;134(B): 249–258 [51]

sue from salvageable tissue at risk and comparing to the clinical exam; i.e., to determine the "core and penumbra." Since brain tissue in the penumbra is dysfunctional, the neurologic exam should reveal impairment in those regions but imaging parameters should suggest viability. Ideally, prompt reperfusion could salvage those tissues and restore neurologic function. Structural imaging, particularly MRI, is extremely valuable, but in the hyperacute setting non-contrast CT may underestimate infarcted tissue since early ischemic changes may take several hours to develop. While DWI is generally considered to reflect the core, it can overestimate infarcted tissue at times due either to heterogeneity of the apparent lesion volume [52] or, rarely through DWI reversal following successful recanalization has been observed [53] (Figs. 15.7 and 15.8).

Commonly accepted thresholds for core infarct and tissue at risk should be treated with skepticism. The relative CBF (rCBF) threshold for the ischemic core is generally recognized as <30% on CTP [55], but a poor signal-to-noise ratio can result in unreliable measure of core infarct volume [56]. Decreased CBF can also be seen in the penumbra so cannot be used in isolation to measure core. Low CBV (<40% of normal) is also used as a measure of core infarct through CBF measures may perform better [53]. Increased time domain parameters (TTP, MTT, T_{max}) can also be used to predict tissue fate, but they are complicated by variability across imaging modalities. Additionally, the route of blood to the ischemic area cannot be determined using these methods, so prolonged time parameters may simply reflect delayed flow through small collaterals to regions with adequate CBF and salvageable tissue.

Among time parameters for penumbra, T_{max} is the most studied, with different cutoffs resulting in higher or lower sensitivity and specificity. Time parameters need to be paired with other measures, such as CBV, for proper interpretation. High T_{max} and low CBV likely represent core infarct while high T_{max} and normal or elevated CBV suggest penumbra. Elevated CBV in the context of prolonged T_{max} is likely a result of autoregulatory vasodilation and increased collateral flow [57]. In chronic occlusive conditions such as intracranial atherosclerotic disease or

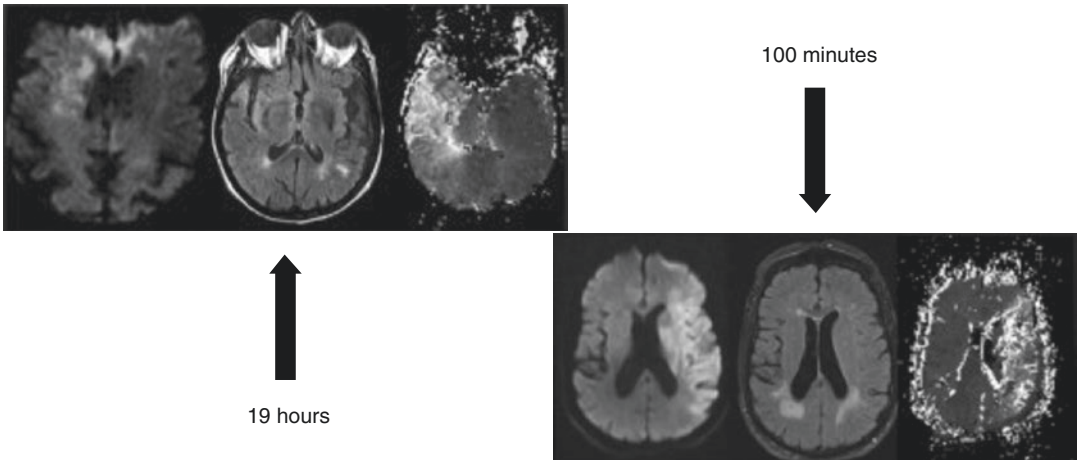

Fig. 15.7 DWI lesion poorly correlates with time of onset. Detailed imaging of acute middle cerebral artery stroke (left to right: diffusion-weighted imaging, fluid-attenuated inversion recovery, time-to-peak perfusion magnetic resonance imaging) shows that one cannot tell time from images. Ann Neurol. 2009 Nov; 66(5):574–590 [54]

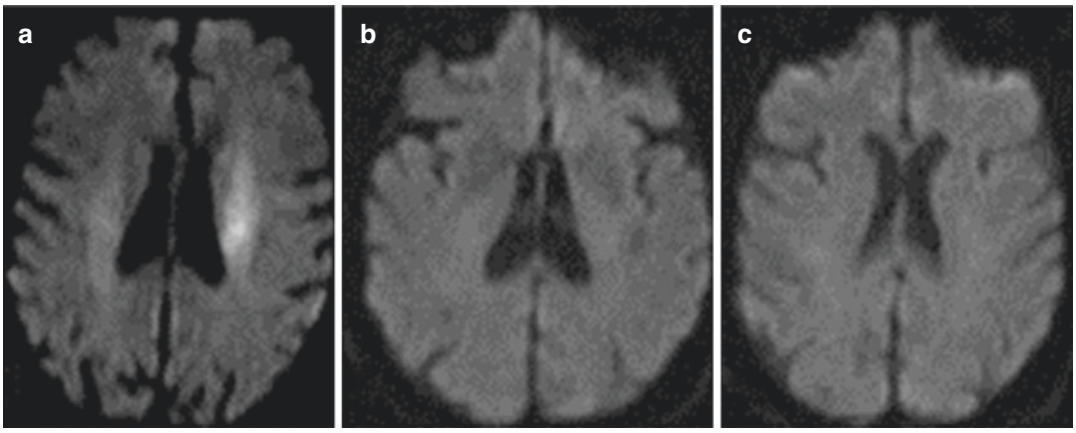

Fig. 15.8 DWI Reversal. Serial diffusion-weighted imaging of acute left middle cerebral artery occlusion shows an initial subcortical abnormality (**a**) and complete reversal (**b**, **c**) 5 days after treatment with intravenous thrombolysis. Ann Neurol. 2009 Nov;66(5):574–590 [54]

moyamoya syndrome, time parameters may be very prolonged without imaging evidence of infarction or with reperfusion outcomes that are better than would be expected based on criteria used in delayed endovascular intervention trials such as DEFUSE [58, 59] (Fig. 15.9).

Beyond the intricacies of the imaging sequences, there are also practical limitations to consider. Inaccurate or misleading perfusion maps can result from numerous scenarios such as poor cardiac output, atrial fibrillation, proximal arterial stenosis, seizures, suboptimal placement of arterial and venous density regions of interest, and other case-specific confounders.

In short, imaging techniques for measuring core and penumbra are not yet sophisticated enough for complete automation and require careful interpretation by clinicians with knowledge of the clinical situation. They also represent a single snapshot in time of a complex and dynamic process that is subject to change, both spontaneously and through medical intervention (Fig. 15.10).

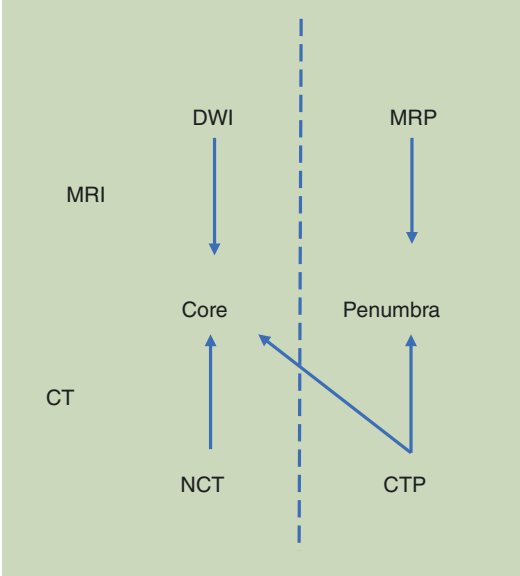

Fig. 15.9 Prediction of core from CT and MRI. MRI predicts core using structural imaging (DWI) and perfusion using MRP. In contrast, CTP uses both structural and perfusion imaging to predict core

15.3 Core and Penumbra

The concept of core and penumbra attempts to model the evolution of acute ischemic stroke and identify individuals who would—or would not—benefit from recanalization therapies. The model is useful for conceptualizing stroke, but in its simplest form relies on a number of assumptions that are rare in clinical practice—for instance, that the lesion is ovoid, homogenous, static, and predictably progressive. The model prompted attempts to develop universally applicable, quantifiable measures and discrete cutoffs for key structural and perfusion imaging variables that have resulted in conflicting results, uncovering the model's shortcomings. The stages of hemodynamic failure introduced previously do not unfold stepwise in clinical practice; the trajectory of hemodynamic compromise is nonlinear and difficult to predict.

IMAGING	CORE	TISSUE AT RISK (PENUMBRA)	ADVANTAGES	DISADVANTAGES
MRI	DWI ADC < 650 FLAIR	FLAIR vascular hyperintensity (slow flow) GRE susceptibility artifact in leptomeningeal vessels	High sensitivity of DWI and good correlation with final infarct volume Clues to time of stroke onset Assessment of stroke mechanism	Occasional overestimation of infarct core with reversibility of initial DWI lesion Rare DWI negative stroke more common in hyperacute phase
CT	ASPECTS	None	Easy to use Widely available	Low inter-rater reliability Radiation +/- contrast
CTA	CT ASPECTS	Collateral status	More direct assessment of LMF Time-resolved multiphase and dynamic CTA has higher interrater agreement	Requires post-processing and whole-brain perfusion CT for dynamic CTA Radiation +/- contrast
CTP & MRP	CT: ASPECTS, Low CBV, rCBF<30% MRI: DWI	Tmax elevated CBV preserved or elevated	Quantitative	Requries contrast Requires post-processing CBF poor indicator of core Limited use in posterior fossa
Nuclear scans: PET, SPECT	CBF below 10 ml/100gr/min	CBF between 10-17 ml/100gr/min OEF elevated CMRO2 preserved or diminished	Gold standard for penumbral imaging Quantitative	Needs nuclear radiotracer subjective measurements Not readily available
DSA	None	Time of maximal opacification Collateral status	Real-time collateral imaging Direct visualization of site of occlusion	Invasive Radiation Contrast dye

Fig. 15.10 Summary of imaging modalities for predicting core and penumbra

When arterial occlusion or clinically significant stenosis occurs, regional CBF transiently decreases. Even in cases of radiographically complete occlusion diminutive flow routes may persist, allowing for thrombolytic access to the clot [54]. The initial fall in CBF is followed rapidly by a compensatory increase in CBV with restoration of CBF, predominantly through the collateral circulation. Collateral circulation may be sufficient to prevent infarction but in many cases of acute stroke the collaterals eventually fail for reasons that are poorly understood. Tissue infarction is a product of both the degree and duration of ischemia, and the magnitude of infarction is modified by patient-level variables, as described above (e.g., age, prior status of cerebral vasculature and tissue, comorbidities, medications, etc.). The "core" is likely better understood as heterogeneous, discontinuous, evolving tissue regions that are most susceptible to ischemia at a given time and fail to recover even if reperfusion occurs. The penumbra regions are similarly heterogeneous and dynamic but are relatively less susceptible to infarction and potentially salvageable, either through intrinsic compensation or therapeutic intervention. A third region of "benign oligemia" with altered CBF but low likelihood for infarction has been proposed. However, it is not strictly oligemic, since CBV may be normal or even elevated, nor is it benign. The third region is best conceptualized as a reflection of the abnormal regional hemodynamics induced by stroke [59].

Tissue changes, venous hemodynamics, and microcirculation also contribute to the evolution of an ischemic stroke. Impaired arterial flow and increased tissue pressure from cytotoxic edema can lead to venous collapse around the area of a stroke [60–62], further exacerbating impairment of blood flow, increasing edema, and potentially raising the risk of hemorrhagic conversion. Increased tissue pressure in the areas of core infarction leads to redirected blood flow to the surrounding tissues with lower tissue pressure, a process known as the cerebral venous steal phenomenon. This process may be a cause of secondary brain injury in stroke and expansion of the ischemic lesion [63]. Poor venous outflow around infarcted tissue correlates with poor arterial collateral flow, demonstrating the important interaction between collaterals, venous congestion, and microcirculation. Whether the driving mechanism is increased tissue pressure and impaired venous outflow, poor collaterals, or, more likely, a combination, is difficult to delineate but the relationship appears clinically significant. In primate models of MCA ischemic stroke, the presence of flow in draining cortical veins was associated with smaller infarct volumes [64]. Increasing venous pressure to avoid collapse in areas at risk for infarction, perhaps by enhancing collaterals, may reduce flow diversion by maintaining patency of outflow tracts, though with the risk of increasing cerebral edema [62] (Fig. 15.11).

Alterations in the capillaries also play a role in stroke evolution [65]. Capillary flow in the brain is heterogeneous but can become more homogenous, leading to greater oxygen extraction efficiency in response to increased oxygen demands. In stroke, dysfunctional or constricted capillaries, if widespread, may lead to greater tissue resistance and persistent ischemia even after arterial reperfusion; one possible cause of the "no reflow" phenomenon after tPA or mechanical thrombectomy. However, decreased flow from higher resistance through these narrowed capillaries may be partially compensated for by increased time for oxygen extraction [66]. Alternately, reactive vasodilation and hyperemia increase abnormal high velocity flow through open capillaries and lead to functional shunting and paradoxical reduction in tissue oxygenation akin to luxury perfusion. It thus appears that capillary dysfunction is of two sorts and can worsen ischemic stroke either by further impairing regional CBF or, paradoxically, by regionally excessive increase of CBF with deleterious reduction in oxygen extraction. Common risk factors for stroke, such as aging, hypertension, diabetes mellitus, Alzheimer's disease, and nicotine use, etc. impair capillary reactivity. Absence of chronic microvascular changes due to these comorbidities in animal models may explain some of the differences between animal models of stroke and clinical

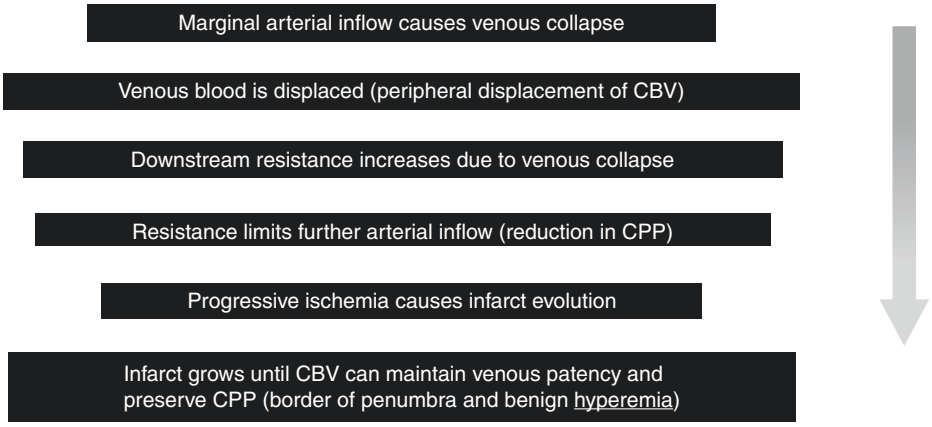

Fig. 15.11 Hypothetical model of infarct progression. Progressive changes in ischemic pathophysiology (arrow from top to bottom), including venous factors that affect cerebral blood volume (CBV) and cerebral perfusion pressure (CPP). Peripheral zones are spared from infarction because of benign hyperemia, characterized by increased CBV. Ann Neurol. 2009 Nov;66(5):574–590 [54]

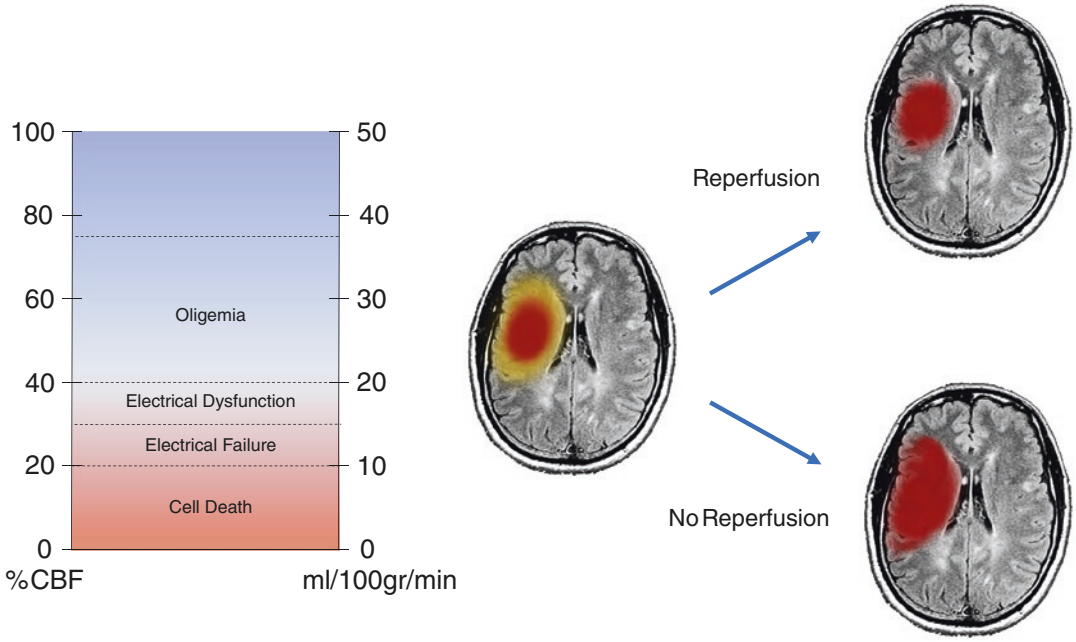

Fig. 15.12 Traditional model of simplified core and penumbra and fixed ischemic thresholds. In this model, the ischemic lesion is assumed to be ovoid, homogenous, static and predictably progressive. Ischemic thresholds are assumed to be fixed. Red shade represents predicted core infarct area. Yellow shade predicts penumbra which behaves reliably by recovering if reperfused or fully infracting without reperfusion

experience; in many cases, stroke in humans may be more accurately described as an acute decompensation of a chronic process [64] (Figs. 15.12 and 15.13).

The dynamic nature of core and penumbra is further illustrated by the subset of patients with fluctuating symptoms. Spontaneous improvement or worsening can result from a variety of

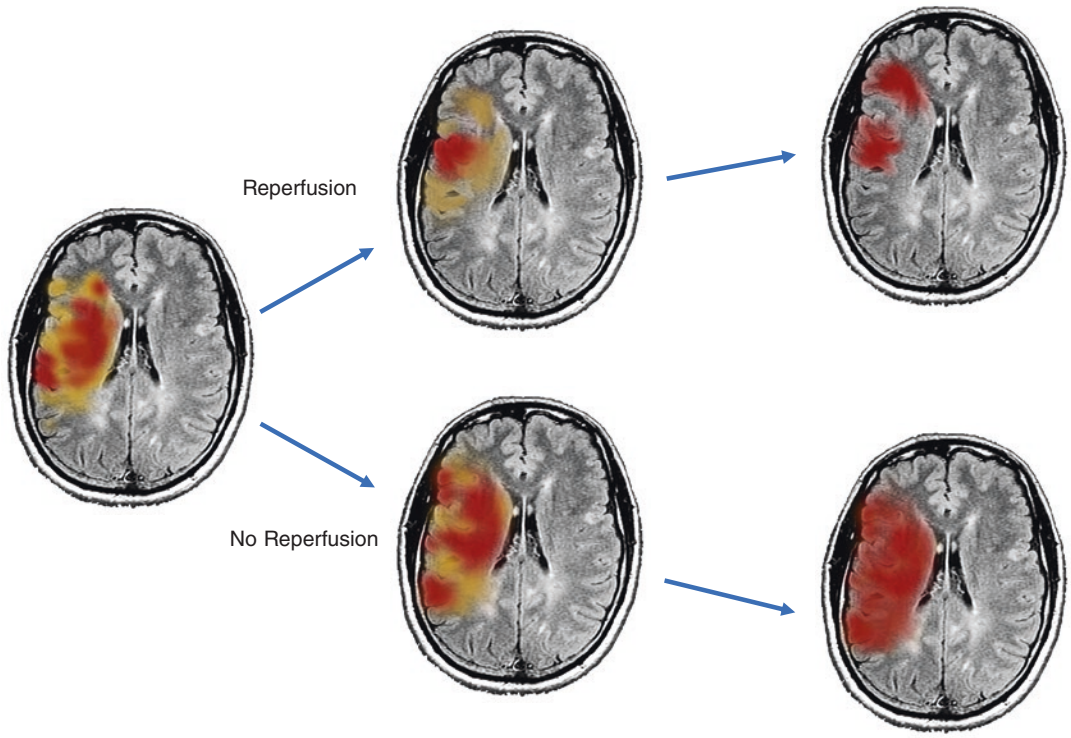

Fig. 15.13 Proposed model of complex core and penumbra. Yellow shade represents predicted penumbra and red shade represents predicted core. Both core and penumbra in this model are discontinuous, heterogenous, and variable. Early predictions of both cores and penumbras can be incorrect and evolve with time. Hazy shading for preliminary and final predicted core areas depict heterogeneous tissue fates within regions of infarction

factors that alter CBF, including spontaneous recanalization, distal embolization or thrombus propagation, reocclusion, and fluctuations in collateral flow. In a subset of patients this can even be affected by upright versus supine head positioning; presumably with patients who have borderline collateral compensation [67].

The mantra "time is brain," like core and penumbra, may apply at the population level, but there is significant variability at the patient level. For one, true time of onset of vessel occlusion should be considered an unknown since in many cases symptoms likely start only when, or if, collaterals fail, rather than at the moment of obstruction. Mechanism of stroke, status of collaterals, premorbid conditions that affect vessel physiology and microcirculation, as well as individual patient factors will influence how quickly or slowly strokes progress. Diffusion lesion size has been shown to correlate poorly with time from stroke onset (see Fig. 15.7) [68]. In a review of patients who underwent thrombectomy, more rapid time to reperfusion increased the odds of a favorable outcome in patients with poor collaterals but was not significantly associated with favorable outcomes in patients with robust collaterals [69]. This suggests that many patients with large vessel occlusion and robust collaterals appear to have a period of relative stability in infarct volume during the initial hours following symptom onset; without recanalization these patients would likely worsen as collateral compensation fails. In contrast, patients with poor collaterals on imaging tend to progress rapidly (Fig. 15.14).

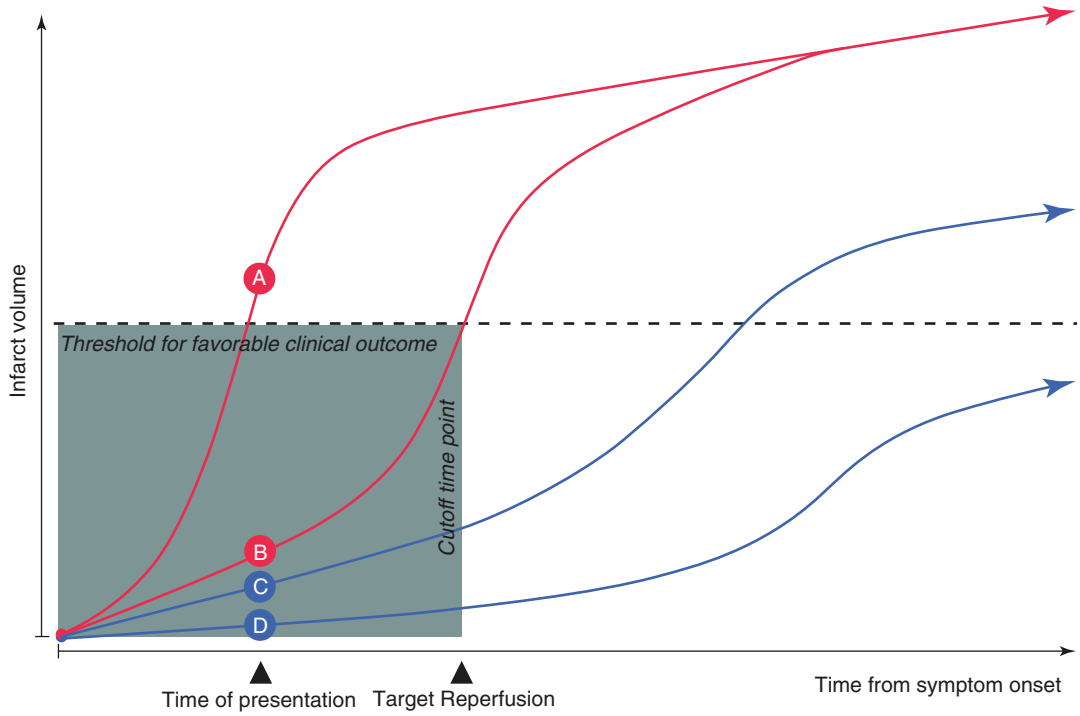

Fig. 15.14 Time is brain but relativity applies. Simplified illustration, which represents the unique effect of time-to-reperfusion on clinical outcome based on proposed collateral scenarios. (A) Universally poor collaterals, which may show large infarcts and severe neurologic deficits at the time of presentation. (B) Rapidly failing collaterals, which may show small-to-medium infarcts and severe neurologic deficits at the time of presentation. (C) Slowly failing collaterals, which may show small infarcts and moderate-to-severe neurologic deficits at the time of presentation. (D) Universally good collaterals, which may show tiny-to-small infarcts and mild-to-moderate neurologic deficits at the time of presentation. In real clinical practice, patients in scenarios B and C can be ideal candidates for endovascular reperfusion. However, the clinical outcome is limited by time-to-reperfusion in scenario B. AJNR 2015;36:495–500 [69]

15.4 Conclusions

Attempts to quantify cerebral blood flow in terms of ischemic thresholds have resulted in overly simplistic models with limited real-world applicability. Unfortunately, core and penumbra cannot yet be reduced to single numerical values. Prior and current attempts to quantify stroke imaging parameters highlight the disconnect between traditional models of ischemia that emphasize arterial occlusion and the more complicated factors that ultimately determine the subsequent perfusion delays and tissue fate. Collateral flow, venous hemodynamics, and microcirculation are major determinants of core and penumbra but are frankly too complicated to be incorporated routinely in acute stroke decision-making algorithms using current imaging modalities.

Spatial and temporal features of stroke have not been properly considered. Current CBF measures provide only a snapshot of a highly dynamic process; they offer only hint at past and future hemodynamic failure or compensation. Structural and perfusion imaging also fail to capture the heterogeneity of both core and penumbra. Definitions of core and penumbra need to take into account whether intervention will be pursued or not since that drastically changes how the lesions will evolve.

Multimodal stroke imaging with structural and CBF measures provides a set of diagnostic tools to offer valuable guidance in acute hemodynamic compromise but major limitations persist. Predicted core and penumbra are far from certain and should not be viewed as a sealed fate. The current automated processes still require real-time expert interpretation. More sophisticated models are needed to move stroke care beyond simplistic models of sequential cascade, rigid thresholds, and linear time course of ischemia in the brain. Until then, delivering optimal precision medicine for acute stroke patients requires clinical acumen, in-depth understanding of the underlying pathophysiology including the complexities of cerebral hemodynamics, and the ability to formulate nuanced interpretations of complex neuroimaging.

References

1. Liebeskind DS, Caplan LR. Intracranial arteries - anatomy and collaterals. Front Neurol Neurosci. 2016;40:1–20.
2. Wollman H, Smith TC, Stephen GW, et al. Effects of extremes of respiratory and metabolic alkalosis on cerebral blood flow in man. J Appl Physiol. 1968;24:60–5.
3. Raichle ME, Posner JB, Plum F. Cerebral blood flow during and after hyperventilation. Arch Neurol. 1970;23:394–403.
4. Dawson SL, Panerai RB, Potter JF. Serial changes in static and dynamic cerebral autoregulation after acute ischaemic stroke. Cerebrovasc Dis. 2003;16:69–75.
5. Shimojyo S, Scheinberg P, Kogure K, et al. The effects of graded hypoxia upon transient cerebral blood flow and oxygen consumption. Neurology. 1968;18:127–33.
6. Dirnagl U, Pulsinelli W. Autoregulation of cerebral blood flow in experimental focal brain ischemia. J Cereb Blood Flow Metab. 1990;10:327–36.
7. Strandgaard S. Autoregulation of cerebral blood flow in hyper-tensive patients. The modifying influence of prolonged antihypertensive treatment on the tolerance to acute, drug-induced hypotension. Circulation. 1976;53:720–7.
8. Powers WJ, Videen TO, Diringer MN, et al. Autoregulation after ischaemic stroke. J Hypertens. 2009;27:2218–22.
9. Nazir FS, Overell JR, Bolster A, et al. Effect of perindopril on cerebral and renal perfusion on normotensives in mild early ischaemic stroke: a randomized controlled trial. Cerebrovasc Dis. 2005;19:77–83.
10. Nazir FS, Overell JR, Bolster A, et al. The effect of losartan on global and focal cerebral perfusion and on renal function in hypertensives in mild early ischaemic stroke. J Hypertens. 2004;22:989–95.
11. Lipsitz LA, Mukai S, Hamner J, Gagnon M, Babikian V. Dynamic regulation of middle cerebral artery blood flow velocity in ageing and hypertension. Stroke. 2000;31:1897–903.
12. Maruyama M, Shimoji K, Ichikawa T, et al. The effects of extreme hemodilutions on the autoregulation of cerebral blood flow, electroencephalogram and cerebral metabolic rate of oxygen in the dog. Stroke. 1985;16:675–9.
13. Haggendal E, Johansson B. Effect of arterial carbon dioxide tension and oxygen saturation on cerebral blood flow autoregulation in dogs. Acta Physiol Scand. 1965;66:27–53.
14. Powers WJ, Press GA, Grubb RL Jr, et al. The effect of hemodynamically significant carotid artery disease on the hemodynamic status of the cerebral circulation. Ann Intern Med. 1987;106:27–34.
15. Heiss WD, Huber M, Fink GR, et al. Progressive derangement of periinfarct viable tissue in ischemic stroke. J Cereb Blood Flow Metab. 1992;12:193–203.
16. An H, Ford A, Chen Y, et al. Early perfusion instability pro-foundly impacts tissue outcome in acute ischemic stroke. In: 2013 International Stroke Conference Oral Abstracts 2013; Abstract 182.
17. Furlan M, Marchal G, Viader F, et al. Spontaneous neurological recovery after stroke and the fate of the ischemic penumbra. Ann Neurol. 1996;40:216–26.
18. Shimosegawa E, Hatazawa J, Ibaraki M, et al. Metabolic penumbra of acute brain infarction: a correlation with infarct growth. Ann Neurol. 2005;57:495–504.
19. Molina CA, Montaner J, Abilleira S, et al. Timing of spontaneous recanalization and risk of hemorrhagic transformation in acute cardioembolic stroke. Stroke. 2001;32:1079–84.
20. Baron JC, Bousser MG, Comar D, et al. Noninvasive tomographic study of cerebral blood flow and oxygen metabolism in vivo. Potentials, limitations, and clinical applications in cerebral ischemic disorders. Eur Neurol. 1981;20:273–84.
21. Astrup J, Siesjö BK, Symon L. Thresholds in cerebral ischemia - the ischemic penumbra. Stroke. 1981;12(6):723–5.
22. Bandera E, Botteri M, Minelli C, Sutton A, Abrams KR, Latronico N. Cerebral blood flow threshold of ischemic penumbra and infarct core in acute ischemic stroke: a systematic review. Stroke. 2006;37:1334–9.
23. Heiss WD, Rosner G. Functional recovery of cortical neurons as related to degree and duration of ischemia. Ann Neurol. 1983;14:294–301.
24. Hossmann KA. Pathophysiology and therapy of experimental stroke. Cell Mol Neurobiol. 2006;26:1057–83.
25. Ní Chróinín D, Asplund K, Åsberg S, Callaly E, Cuadrado-Godia E, Díez-Tejedor E, Di Napoli M, Engelter ST, Furie KL, Giannopoulos S, Gotto AM

Jr, Hannon N, Jonsson F, Kapral MK, Martí-Fàbregas J, Martínez-Sánchez P, Milionis HJ, Montaner J, Muscari A, Pikija S, Probstfield J, Rost NS, Thrift AG, Vemmos K, Kelly PJ. Statin therapy and outcome after ischemic stroke: systematic review and meta-analysis of observational studies and randomized trials. Stroke. 2013;44(2):448–56. https://doi.org/10.1161/STROKEAHA.112.668277.
26. Meng R, Asmaro K, Meng L, Liu Y, Ma C, Xi C, Li G, Ren C, Luo Y, Ling F, Jia J, Hua Y, Wang X, Ding Y, Lo EH, Ji X. Upper limb ischemic preconditioning prevents recurrent stroke in intracranial arterial stenosis. Neurology. 2012;79(18):1853–61. https://doi.org/10.1212/WNL.0b013e318271f76a.
27. Bang OY, Park HY, Lee PH, Kim GM, Chung CS, Lee KH. Improved outcome after atherosclerotic stroke in male smoker. J Neurol Sci. 2007;260(1–2):43–8.
28. Kang CG, Chun MH, Kang JA, Do KH, Choi SJ. Neurocognitive dysfunction according to hypoperfusion territory in patients with Moyamoya disease. Ann Rehabil Med. 2017;41(1):1–8. https://doi.org/10.5535/arm.2017.41.1.1.
29. Calviere L, Catalaa I, Marlats F, Januel AC, Lagarrigue J, Larrue V. Improvement in cognitive function and cerebral perfusion after bur hole surgery in an adult with moyamoya disease. Case report. J Neurosurg. 2011;115(2):347–9. https://doi.org/10.3171/2011.3.JNS101117.
30. Liebeskind DS. Collateral circulation. Stroke. 2003;34:2279–84.
31. Wei L, Erinjeri JP, Rovainen CM, Woolsey TA. Collateral growth and angiogenesis around cortical stroke. Stroke. 2001;32:2179–84.
32. Manoonkitiwongsa PS, Jackson-Friedman C, McMillan PJ, Schultz RL, Lyden PD. Angiogenesis after stroke is correlated with increased numbers of macrophages: the clean-up hypothesis. J Cereb Blood Flow Metab. 2001;21:1223–31.
33. Caplan LR, Hennerici M. Impaired clearance of emboli (washout) is an important link between hypoperfusion, embolism, and ischemic stroke. Arch Neurol. 1998;55:1475–82.
34. Kucinski T, Koch C, Eckert B, Becker V, Kromer H, Heesen C, Grzyska U, Freitag HJ, Rother J, Zeumer H. Collateral circulation is an independent radiological predictor of outcome after thrombolysis in acute ischaemic stroke. Neuroradiology. 2003;45:11–8.
35. Hedera P, Bujdáková J, Traubner P, Pancák J. Stroke risk factors and development of collateral flow in carotid occlusive disease. Acta Neurol Scand. 1998;98(3):182–6.
36. Kim SK, Wang KC, Kim IO, Lee DS, Cho BK. Combined encephaloduroarteriosynangiosis and bifrontal encephalogaleoperiostealsynangiosis in pediatric moyamoya disease. Neurosurgery. 2002;50:88–96.
37. Makkat S, Stadnik T, Peeters E, et al. Pathogenesis of venous stroke: evaluation with diffusion- and perfusion-weighted MRI. J Stroke Cerebrovascular Dis. 2003;12:132–6.
38. Frerichs KU, Deckert M, Kempski O, et al. Cerebral sinus and venous thrombosis in rats induces long-term deficits in brain function and morphology: evidence for a cytotoxic genesis. J Cereb Blood Flow Metab. 1994;14:289–300.
39. Röttger C, Trittmacher S, Gerriets T, et al. Reversible MR imaging abnormalities following cerebral venous thrombosis. AJNR Am J Neuroradiol. 2005;26:607–13.
40. Schaller B, Graf R. Cerebral venous infarction: the pathophysiological concept. Cerebrovasc Dis. 2004;18(3):179–88.
41. Schuchardt F, Hennemuth A, Schroeder L, Meckel S, Markl M, Wehrum T, Harloff A. Acute cerebral venous thrombosis: three-dimensional visualization and quantification of hemodynamic alterations using 4-dimensional flow magnetic resonance imaging. Stroke. 2017;48(3):671–7. https://doi.org/10.1161/STROKEAHA.116.015102.
42. Gisolf J, van Lieshout JJ, van Heusden K, Pott F, Stok WJ, Karemaker JM. Human cerebral venous outflow pathway depends on posture and central venous pressure. J Physiol. 2004;560(Pt 1):317–27. https://doi.org/10.1113/jphysiol.2004.070409.
43. Heiss WD. Radionuclide imaging in ischemic stroke. J Nucl Med. 2014;55(11):1831–41.
44. Feeney DM, Baron JC. Diaschisis. Stroke. 1986;17:817–30.
45. Sobesky J, Thiel A, Ghaemi M, et al. Crossed cerebellar diaschisis in acute human stroke: a PET study of serial changes and response to supratentorial reperfusion. J Cereb Blood Flow Metab. 2005;25:1685–91.
46. Rijntjes M, Weiller C. Recovery of motor and language abilities after stroke: the contribution of functional imaging. Prog Neurobiol. 2002;66:109–22.
47. Murase N, Duque J, Mazzocchio R, Cohen LG. Influence of interhemispheric interactions on motor function in chronic stroke. Ann Neurol. 2004;55:400–9.
48. Heiss WD, Thiel A, Winhuisen L, Mühlberger B, Kessler J, Herholz K. Functional imaging in the assessment of capability for recovery after stroke. J Rehabil Med. 2003;41:27–33.
49. Hsu WY, Cheng CH, Liao KK, Lee IH, Lin YY. Effects of repetitive transcranial magnetic stimulation on motor functions in patients with stroke: a meta-analysis. Stroke. 2012;43:1849–57.
50. Thiel A, Hartmann A, Rubi-Fessen I, et al. Effects of noninvasive brain stimulation on language networks and recovery in early poststroke aphasia. Stroke. 2013;44:2240–6.
51. Hosseini MB, Liebeskind DS. The role of neuroimaging in elucidating the pathophysiology of cerebral ischemia. Neuropharmacology. 2018;134(B):249–58.
52. del Zoppo GJ, Sharp FR, Heiss WD, Albers GW. Heterogeneity in the penumbra. J Cereb Blood Flow Metab. 2011;31(9):1836–51. https://doi.org/10.1038/jcbfm.2011.93.
53. Kranz PG, Eastwood JD. Does diffusion-weighted imaging represent the ischemic core? An evidence-

based systematic review. Am J Neuroradiol. 2009;30:1206–12.
54. Liebeskind DS. Imaging the future of stroke: I. Ischemia. Ann Neurol. 2009;66(5):574–90. https://doi.org/10.1002/ana.21787.
55. Yu Y, Han Q, Ding X, Chen Q, Ye K, Zhang S, Yan S, Campbell BC, Parsons MW, Wang S, Lou M. Defining core and penumbra in ischemic stroke: a voxel- and volume-based analysis of whole brain CT perfusion. Sci Rep. 2016;6:20932.
56. Schaefer PW, Souza L, Kamalian S, Hirsch JA, Yoo AJ, Kamalian S, Gonzalez RG, Lev MH. Limited reliability of computed tomographic perfusion acute infarct volume measurements compared with diffusion-weighted imaging in anterior circulation stroke. Stroke. 2015;46:419–24.
57. Srinivasan A, Goyal M, Al Azri F, et al. State-of-the-art imaging of acute stroke. Radiographics. 2006;26(Suppl 1):S75–95.
58. Bang OY, Kwang HL, Suk JK, Liebeskind DS. Benign oligemia despite a malignant MRI profile in acute ischemic stroke. J Clin Neurol. 2010;6(1):41–5.
59. Calamante F, Ganesan V, Kirkham FJ, Jan W, Chong WK, Gadian DG, Connelly A. MR perfusion imaging in Moyamoya syndrome: potential implications for clinical evaluation of occlusive cerebrovascular disease. Stroke. 2001;32:2810–6.
60. Kulik T, Kusano Y, Aronhime S, et al. Regulation of cerebral vasculature in normal and ischemic brain. Neuropharmacology. 2008;55:281–8.
61. del Zoppo GJ, Hallenbeck JM. Advances in the vascular pathophysiology of ischemic stroke. Thromb Res. 2000;98:73–81.
62. Ursino M, Lodi CA. A simple mathematical model of the interaction between intracranial pressure and cerebral hemodynamics. J Appl Physiol (1985). 1997;82:1256–69.
63. Pranevicius M, Pranevicius O. Cerebral venous steal: blood flow diversion with increased tissue pressure. Neurosurgery. 2002;51(5):1267–73.. discussion 1273-4
64. Sasaki M, Honmou O, Radtke C, et al. Development of a middle cerebral artery occlusion model in the nonhuman primate and a safety study of i.v. infusion of human mesenchymal stem cells. PLoS One. 2011;6:e26577.
65. Østergaard L, Jespersen SN, Engedahl T, Jiménez EG, Ashkanian M, Hansen MB, Eskildsen S, Mouridsen K. Capillary dysfunction: its detection and causative role in dementias and stroke. Curr Neurol Neurosci Rep. 2015;15(6):37. https://doi.org/10.1007/s11910-015-0557-x.
66. Dalkara T, Arsava EM. Can restoring incomplete microcirculatory reperfusion improve stroke outcome after thrombolysis? J Cereb Blood Flow Metab. 2012;32:2091–9.
67. Ali LK, Weng JK, Starkman S, Saver JL, Kim D, Ovbiagele B, Buck BH, Sanossian N, Vespa P, Bang OY, Jahan R, Duckwiler GR, Viñuela F, Liebeskind DS. Heads up! A novel provocative maneuver to guide acute ischemic stroke management. Interv Neurol. 2017;6(1–2):8–15. https://doi.org/10.1159/000449322.
68. Hakimelahi R, Vachha BA, Copen WA, Papini GD, He J, Higazi MM, Lev MH, Schaefer PW, Yoo AJ, Schwamm LH, González RG. Time and diffusion lesion size in major anterior circulation ischemic strokes. Stroke. 2014;45(10):2936–41. https://doi.org/10.1161/STROKEAHA.114.005644.
69. Hwang YH, Kang DH, Kim YW, Kim YS, Park SP, Liebeskind DS. Impact of time-to-reperfusion on outcome in patients with poor collaterals. Am J Neuroradiol. 2015;36(3):495–500. https://doi.org/10.3174/ajnr.A4151.